# Calcium-activated chloride current in normal mouse sympathetic ganglion cells

Fernando De Castro, Emilio Geijo-Barrientos and Roberto Gallego*

*Instituto de Neurociencias y Departamento de Fisiología, Universidad de Alicante, Apartado 374, 03080 Alicante, Spain*

1. In rat sympathetic ganglion cells, axotomy induces the appearance of a depolarizing after-potential (ADP) produced by a calcium-activated chloride current. Here we report that this current is also present in normal sympathetic neurones from the mouse.

2. In an *in vitro* preparation of the superior cervical ganglion, an ADP was observed after spike firing in 50% of the cells studied with single-electrode current- and voltage-clamp techniques.

3. When the cells were voltage clamped at −50 mV in the presence of tetrodotoxin (TTX) and tetraethylammonium chloride (TEA), depolarizing jumps evoked inward calcium currents which were contaminated by outward chloride currents, followed by slowly decaying inward chloride tail currents.

4. The ADP and the inward tail currents disappeared when calcium was removed from the extracellular solution or when cadmium was added.

5. The reversal potential for the inward tail current was approximately −24 mV and was displaced in agreement with the Nernst equation for chloride when the extracellular NaCl was replaced by sucrose or sodium isethionate. The chloride channel blocker anthracene-9-carboxylic acid (9AC) inhibited both the ADP and the tail current.

6. Using intracellular injection of neurobiotin, we found that cells with shorter dendrites had larger ADPs. In axotomized ganglia practically all cells showed very pronounced ADPs.

7. We conclude that normal mouse sympathetic ganglion cells have a calcium-activated chloride current that generates an ADP. The channels responsible for this current are probably located in the dendrites.

The electrical behaviour of a neurone is determined by the type and location of the ion channels present in its membrane. In normal rat sympathetic neurones, action potential firing is always followed by an after-hyperpolarization (AHP) produced by a calcium-dependent potassium conductance (McAfee & Yarowsky, 1979; Belluzzi & Sacchi, 1990; Sacchi, Rossi & Canella, 1995), but several days after axotomy many of these cells show an after-depolarization (ADP) generated by a calcium-activated chloride current (Sánchez-Vives & Gallego, 1993, 1994). In contrast, no ADPs are observed in control or axotomized guinea-pig ganglion cells (Purves, 1975; Sánchez-Vives & Gallego, 1993). One explanation for these differences is that the channels responsible for the ADP in rat ganglion cells are incorporated *de novo* in the membrane as a reaction to axotomy. However, another possibility is that the channels are present in the non-axotomized sympathetic neurone but are located in the distal dendrites, where the effect of their activation on the membrane potential recorded at the cell body would be too small to detect. The dendritic retraction produced by axotomy (Yawo, 1987) would make the ADP visible from the cell body in rat sympathetic neurones, but not in guinea-pig ganglion cells that have longer dendrites (Purves & Lichtman, 1985). Considering the above, a membrane potential change produced by the activation of the chloride conductance would be too small to be recorded from the cell body of normal rat and guinea-pig ganglion cells, but could be seen in mouse sympathetic neurones which have very short dendrites (Purves & Lichtman, 1985). In this paper we demonstrate that normal mouse sympathetic neurones show the calcium-activated chloride current described in axotomized rat ganglion cells and we suggest that the channels responsible for this current are located in the distal dendrites. Part of this work has been presented in abstract form (De Castro, Geijo-Barrientos & Gallego, 1995*a*).

* To whom correspondence should be addressed.

## METHODS

The methods for intracellular and voltage-clamp recording have been described previously (Sánchez-Vives & Gallego, 1993, 1994). Briefly, 8- to 13-week-old mice (Swiss OF-1) were deeply anaesthetized by an I.P. injection of sodium pentobarbitone (40 mg $kg^{-1}$) and perfused through the heart with cold oxygenated saline until breathing stopped. The right superior cervical ganglion was taken from the animal and pinned to the Sylgard (Dow-Corning, Midland, MI, USA) bottom of a chamber that was continuously superfused with saline (mM: NaCl, 128; KCl, 5; $CaCl_2$, 2·5; $MgCl_2$, 1; $NaH_2PO_4$, 1; $NaHCO_3$, 16; glucose, 5·5) equilibrated with 95% $O_2$–5% $CO_2$ (pH 7·4) at room temperature (22–25 °C). The ganglion was illuminated from one side by a fine fibre optic light source, allowing the cells on the surface to be seen using a microscope (×375–600). For all voltage-clamp experiments 1 μM tetrodotoxin (TTX; Sigma) was added to the saline and 25 mM tetraethylammonium chloride (TEA) substituted for NaCl. The low-chloride solutions were made by replacing NaCl with sodium isethionate or sucrose. Anthracene-9-carboxylic acid (9AC; Sigma) or apamin (Sigma) were applied dissolved in the superfusing solution. Potentials were measured with respect to a Ag–AgCl pellet connected to the bath through an agar–KCl bridge. Junction potential shifts due to solution changes were usually smaller than 10 mV and were taken into account when plotting $I$–$V$ curves (for details see Sánchez-Vives & Gallego, 1994). In a group of mice the postganglionic branches of the superior cervical ganglion were cut under pentobarbitone anaesthesia (35 mg $kg^{-1}$, I.P.) 8 days prior to the experiment using aseptic precautions as described previously (Sánchez-Vives & Gallego, 1993, 1994; De Castro, Sánchez-Vivez, Muñoz-Martinez & Gallego, 1995*b*). The experimental procedures were in accordance with the guidelines of the Ethics Committee of the Instituto de Neurociencias de Alicante.

Cells were impaled with microelectrodes filled with 3 M KCl or 3 M potassium acetate and bevelled to a resistance of 40–90 MΩ. Data were collected only if the neurone generated action potentials of at least 70 mV (65 mV for axotomized neurones). The sampling frequency for discontinuous single-electrode voltage clamp was 4–8 kHz, with a duty cycle of 30/70. Capacity compensation was continuously monitored and adjusted to ensure head stage settling. After filtering at 1 kHz, data were digitized and stored in a computer for subsequent analysis using commercial software (Cambridge Electronic Design Limited, Cambridge, UK). In current-clamp experiments, 50 Hz trains of depolarizing pulses (5 ms, 0·5–2 nA) were applied and the membrane potential was measured relative to the resting potential 50 ms after the end of the train. We considered the cell to have shown an ADP when the measured value was 0 or positive, or an AHP if it was negative. The values for the different experimental groups are given as means ± S.E.M. Statistical comparisons were made using Student's $t$ test for means (Sigmastat; Jandel Scientific Software, Erkrath, Germany).

In some cells neurobiotin (Vector Laboratories, Burlingame, CA, USA) was injected after the electrophysiological measurements by

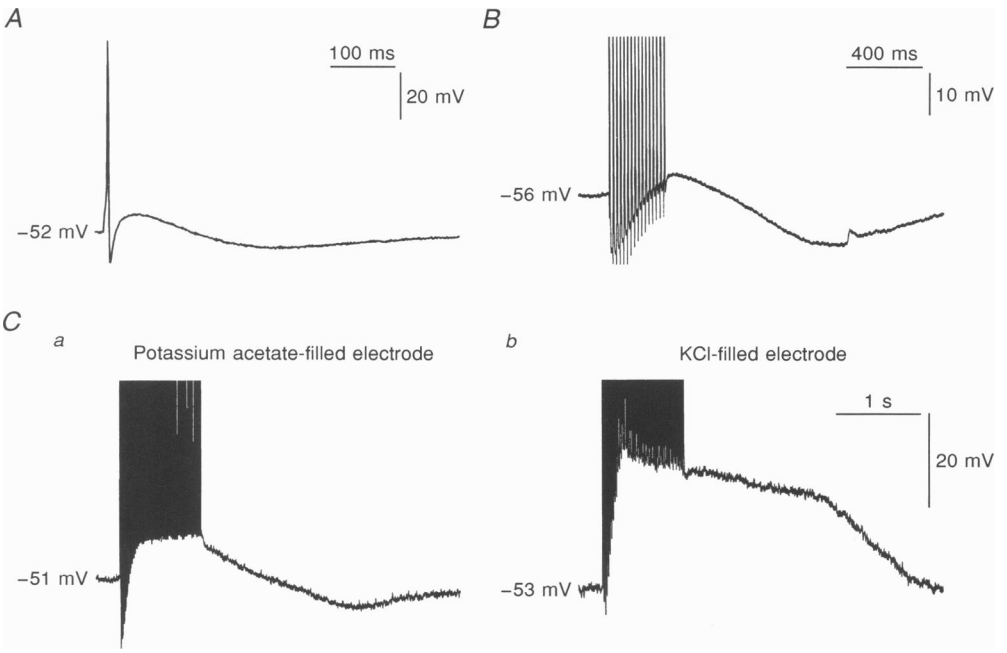


**Figure 1. ADPs recorded in mouse sympathetic ganglion cells**

*A*, a single spike was followed by a small ADP and a prolonged AHP. *B*, another neurone showed an AHP after a single spike but an ADP built up during a train of 16 spikes at 50 Hz and was followed by an AHP. *C*, a neurone was successively impaled with an electrode filled with 3 M potassium acetate (*a*) and with another electrode filled with 3 M KCl (*b*). The ADP evoked by a train of 50 spikes at 50 Hz was markedly increased when recorded with the KCl-filled electrode. In all panels the values to the left are the resting membrane potential ($V_m$). In this and subsequent figures, action potentials were evoked with short (5 ms) intracellular current pulses (0·5–1 nA). Spikes are truncated in *B* and *C*.

applying depolarizing current pulses (300–700 ms, 0·1–0·6 nA, 0·5–1 Hz) over a period of at least 15 min. For these experiments the microelectrode tip was filled with 5% neurobiotin in 1 M KCl and the microelectrode backfilled with 3 M KCl. Microelectrode resistance was 150–200 MΩ. After overnight fixation in paraformaldehyde (4%), ganglia were incubated in 1% (v/v) Triton X-100, reacted with Vectastain kit ABC (Vector Laboratories) and then visualized with diaminobenzidine (Morgan, De Groat, Felkins & Zhang, 1991). Three-dimensional reconstruction of stained cells was performed with a video camera connected to a microscope using the computer program Neurograph (Microptic, Barcelona, Spain). The morphological parameters measured for each neurone included: total dendritic length (the sum of the lengths of all dendritic branches), dendritic branches at 75 μm (the number of dendritic branches that crossed a line traced at 75 μm from the cell body in the computer reconstruction; we chose this value because it was about one-half of the maximum dendritic length in most cells with several long dendrites) and total number of terminal dendritic segments.

# RESULTS

## After-depolarization in mouse sympathetic ganglion cells

In contrast to rat and guinea-pig ganglion cells, non-axotomized sympathetic neurones from the mouse showed ADPs after action potential firing (Fig. 1). When impaled with electrodes filled with 3 M KCl, 3% of the cells ($n = 167$; resting membrane potential ($V_m$) = $-51 \pm 0{\cdot}5$ mV) showed an ADP after firing a single action potential (Fig. 1*A*) and 51% showed an ADP following a train of spikes (Fig. 1*B* and *C*; see also Figs 3, 5 and 7). With this latter form of activation, in most cells the ADP built up from an AHP generated by the first action potentials in the train and was followed by a slow AHP (Figs 1, 3, 5 and 7). When thirty-five spikes were fired at 50 Hz the ADP had an average maximum value of $9 \pm 1$ mV and lasted for $764 \pm 92$ ms ($n = 85$; $V_m = -53 \pm 0{\cdot}8$ mV).

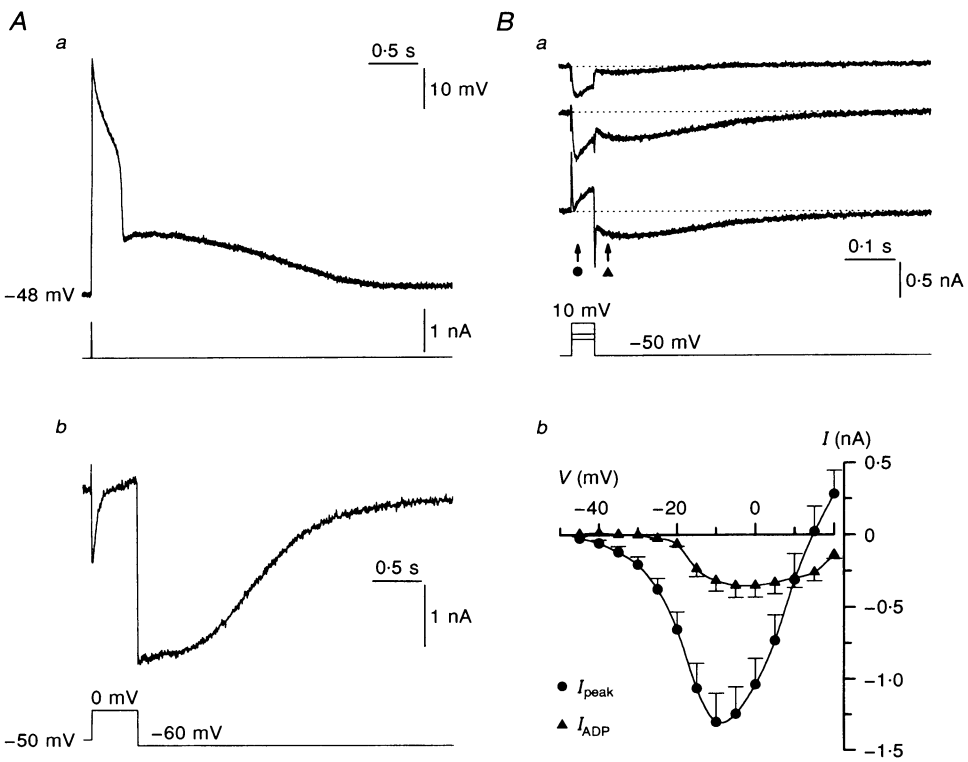


**Figure 2. In the presence of TTX and TEA, depolarizing pulses generated ADPs when in current clamp and inward tail currents when in voltage clamp**

*A a*, a short (10 ms) current pulse triggered a calcium spike followed by a long ADP. $V_m$, −48 mV. *A b*, a depolarizing voltage jump applied to the same cell while in voltage clamp evoked an inward peak ($I_{peak}$) at the beginning of the pulse followed by an outward relaxation and an inward tail current ($I_{ADP}$) upon repolarization. *B a*, samples of the voltage jumps applied to another cell when studying the *I–V* relationship. The inward current recorded during the pulse in the two upper traces (jumps to −20 and −10 mV) becomes mostly outward with the jump to +10 mV. $I_{ADP}$ follows each voltage pulse. Symbols indicate the time at which measurements were made for the *I–V* curves. *B b*, average *I–V* plots for $I_{peak}$ and $I_{ADP}$ obtained from 13 neurones using protocols similar to that shown in *B a*. The bars in this and subsequent figures are 1 S.E.M. In these and all subsequent voltage-clamp recordings, except those in Fig. 4*A a*, leak currents have been subtracted.

The amplitude of the ADP was related to the chloride content of the microelectrode. In twenty-nine cells impaled with 3 M potassium acetate-filled electrodes ($V_m = -55 \pm 1{\cdot}7$ mV) a train at 50 Hz evoked an ADP of only $4 \pm 3$ mV ($P < 0{\cdot}05$, when compared with the value for the 85 cells impaled with KCl-filled electrodes, $t$ test). Furthermore, in thirteen other neurones we recorded successively with an electrode filled with potassium acetate ($V_m = -49 \pm 1{\cdot}4$ mV) and with an electrode filled with KCl ($V_m = -54 \pm 2{\cdot}2$ mV). As shown in Fig. 1*C*, an increase in the amplitude and duration of the ADP following a train of spikes was observed when recording with a KCl-filled electrode. On average, the after-potential was displaced 12 mV in a positive direction when recorded with a KCl-filled electrode, and the duration increased by 1240 ms ($P < 0{\cdot}05$, paired $t$ test). These results suggest that the ADP is produced by activation of a chloride conductance following spike firing and that chloride ions escape from the electrode, increasing the intracellular chloride concentration.

### Voltage clamp of the after-depolarization

In the presence of 1 μM TTX and 25 mM TEA, depolarizing pulses under current clamp produced active responses followed by long ADPs in most cells (Fig. 2*A a*). When the cells were voltage clamped, inward peaks and outward currents were recorded during jumps from −50 to near 0 mV, followed by slowly decaying inward tail currents (Fig. 2*A b*). From now on, we will refer to the inward peak current as $I_{peak}$ and to the inward tail current as $I_{ADP}$, although calcium-activated chloride currents are often abbreviated as $I_{Cl(Ca)}$. $I_{peak}$ was measured by subtracting the leak from the most negative current recorded during the pulse and $I_{ADP}$ as the current value 25 ms after the end of the voltage jump.

Figure 2*B a* shows examples of the currents evoked by 50 ms depolarizing voltage jumps of increasing amplitude from a holding potential of −50 mV. The average $I$–$V$ curves obtained with similar protocols in thirteen neurones show that $I_{peak}$ activated at −35 mV and reached a maximum at about −10 mV and that $I_{ADP}$ activated around −25 mV and decreased slightly with jumps to the most depolarized levels (Fig. 2*B b*). These plots are similar to those obtained from axotomized rat ganglion cells (Sánchez-Vives & Gallego, 1994) and, since there are no TTX-resistant sodium currents in sympathetic neurones (Belluzzi & Sacchi, 1986; Schofield & Ikeda, 1989), the plots suggest that $I_{peak}$ results primarily from a calcium current and that calcium entry

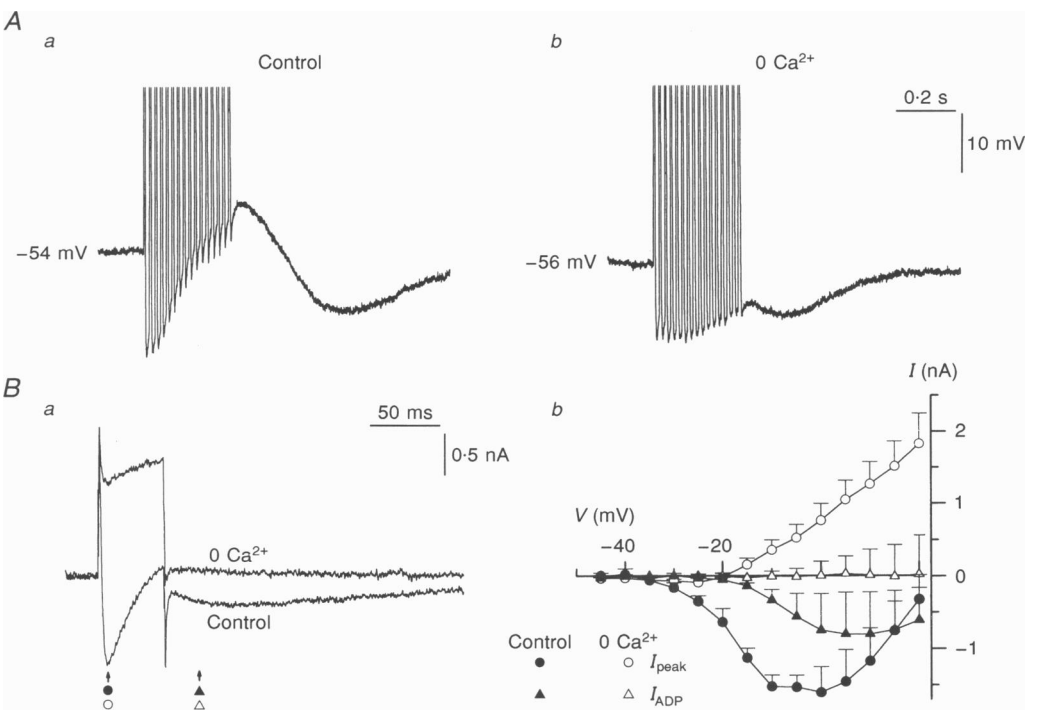


**Figure 3. Extracellular calcium was needed for the generation of the ADP**

*A*, the ADP recorded after a train of 16 spikes in control solution (*a*) practically disappeared when a $Ca^{2+}$-free solution was applied (*b*). Spikes are truncated in both panels. $V_m$ values are shown to the left. *Ba*, inward and tail currents generated by a depolarizing jump to 0 mV from a holding voltage of −50 mV disappeared when the control solution was changed to one without calcium. *B b*, average $I$–$V$ plots for the points indicated by the corresponding symbols in *Ba* show that $I_{ADP}$ disappeared and $I_{peak}$ was replaced by an outward current when calcium was removed ($n = 3$). Control values are the mean of 8 cells.

during the depolarizing pulse activates $I_{ADP}$, which is outward when the membrane potential is positive and inward upon repolarization (Sánchez-Vives & Gallego, 1994; see also Owen, Segal & Barker, 1984; Mayer, 1985; Akasu, Nishimura & Tokimasa, 1990).

### $I_{ADP}$ is a calcium-activated current

As in axotomized sympathetic ganglion cells from the rat (Sánchez-Vives & Gallego, 1993, 1994), the amplitude and duration of the ADP recorded after a train of spikes increased with the number of action potentials in the train

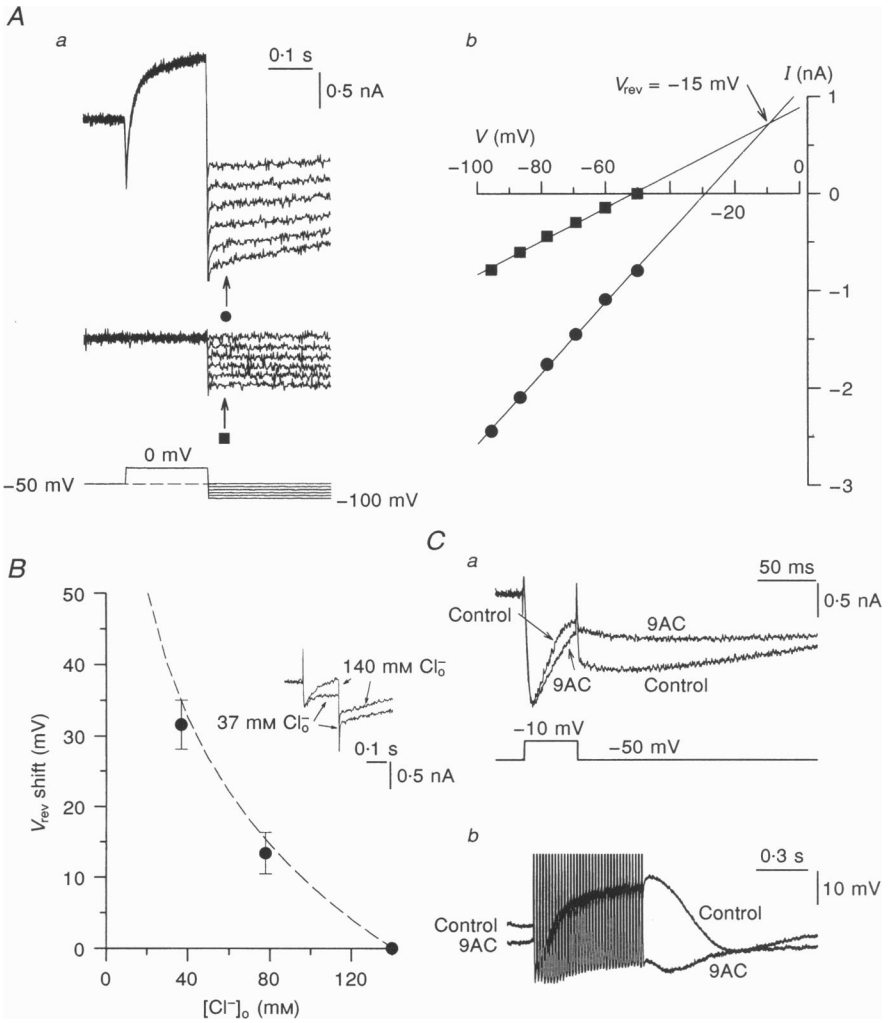


**Figure 4. Chloride dependence of $I_{ADP}$**

*A a*, inward tail currents (upper trace) were evoked by depolarizing jumps to 0 mV and the membrane was repolarized to different levels between −100 and −50 mV (lower trace). When no depolarizing pulse was applied no tail currents were recorded (middle trace). *A b*, *I–V* relationships for the currents measured at the points indicated by the symbols in *a*. The intersection of the two lines corresponds to the extrapolated reversal potential ($V_{rev}$). *B*, plot of the shift in reversal potential for $I_{ADP}$ from the control value obtained in 11 cells when the extracellular concentration of chloride ($[Cl^-]_o$) was 140 mM. The point at 78 mM $Cl^-_o$ is the average shift obtained from 2 sucrose and 2 isethionate substitutions and the point at 37 mM $Cl^-_o$ is the average of 5 sucrose and 2 isethionate substitutions. The dashed line is the predicted change for the chloride equilibrium potential according to the Nernst relation: $V_{rev}$ shift $= 59 \log[Cl^-]_{o1}/[Cl^-]_{o2}$, where $[Cl^-]_{o1}$ is the chloride concentration in the control solution and $[Cl^-]_{o2}$ is the changed chloride concentration. Inset shows currents evoked by a depolarizing jump to 0 mV from −50 mV in control solution ($[Cl^-]_o = 140$ mM) and when NaCl was replaced by sodium isethionate ($[Cl^-]_o = 37$ mM). In the low-chloride solution the amplitude of $I_{ADP}$ increased and the current was inward during the pulse because the chloride reversal potential was positive. *C a*, $I_{ADP}$ evoked by a depolarizing jump to −10 mV decreased to 56% of its control value when the experiment was performed in the presence of the calcium channel blocker 9AC (2 mM), but $I_{peak}$ was not affected. *C b*, in another cell 2 mM 9AC practically abolished the ADP generated by a train of 35 spikes. Spikes are truncated.

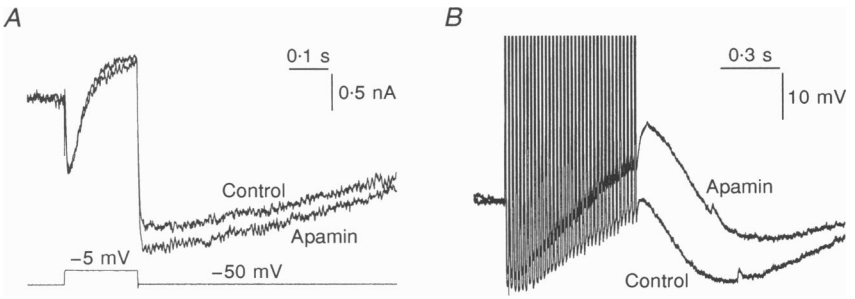


**Figure 5. Effects of the calcium-activated potassium channel blocker apamin on $I_{ADP}$ and on the ADP**

*A*, 0·1 $\mu$M apamin produced a 20% increase in $I_{ADP}$ evoked by a jump to −5 mV from −50 mV. *B*, in another cell 0·1 $\mu$M apamin increased the amplitude of the ADP following a train of 35 spikes. Spikes are truncated.

(not shown), suggesting that the activation of the current was greater when more calcium entered the cell with the longer trains. In support of this view, the ADP was markedly reduced when calcium was removed from the solution ($n = 5$; Fig. 3*A*) and was completely abolished when in addition 1 mM EGTA was added to the extracellular solution ($n = 2$).

$I_{ADP}$ was also dependent on calcium entry during the depolarizing pulse. If calcium was removed from the extracellular medium ($n = 3$; Fig. 3*B a*), or replaced by the calcium channel blocker cadmium (0·2–0·5 mM; $n = 5$; not shown), $I_{peak}$ and $I_{ADP}$ practically disappeared. As can be seen in the average $I$–$V$ plots (Fig. 3*B b*), when calcium entry was impeded an outward current was unmasked during the depolarizing pulses to positive values. Although we have not studied this current, it is probably the time invariant non-specific outward current described in rat sympathetic cells (Belluzzi & Sacchi, 1989). Nevertheless, it

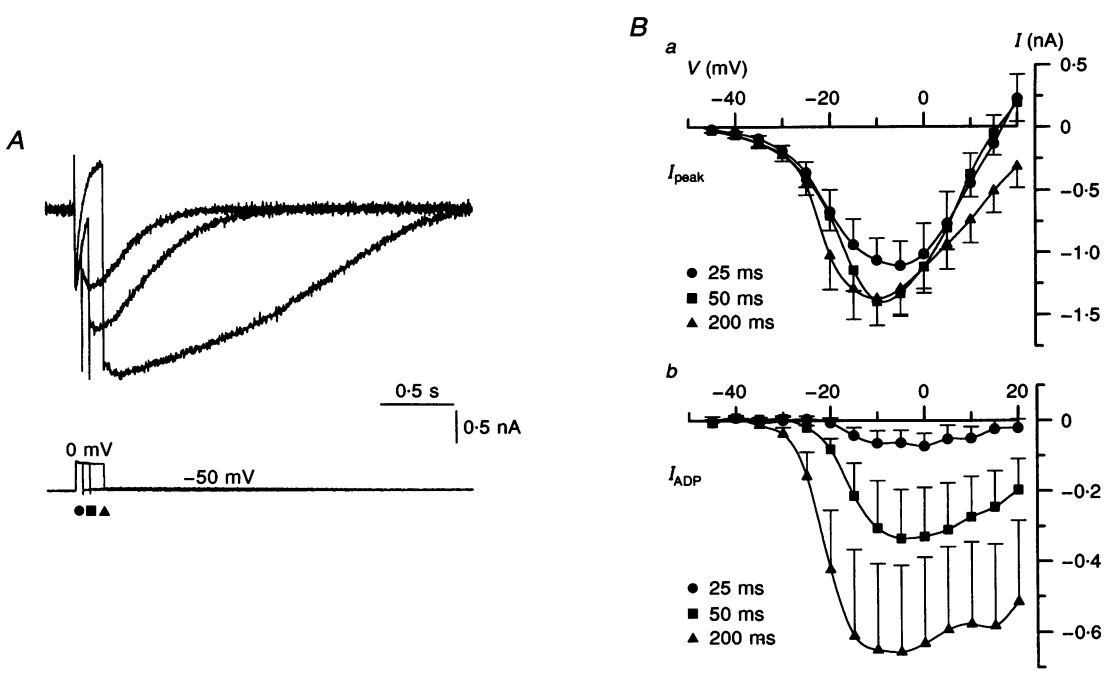


**Figure 6. Effects of increasing pulse duration on $I_{ADP}$**

*A*, the amplitude and duration of $I_{ADP}$ increased when pulses of 25, 50 and 200 ms were applied. When 200 ms pulses were applied the interval between pulses was always greater than 15 s (usually 30 s). Symbols correspond to the different traces in *B*. *B*, average $I$–$V$ plots for 4 cells, in which protocols similar to that shown in *A* were applied, show that $I_{peak}$ did not change with the different pulses (*a*), but $I_{ADP}$ increased in amplitude with the longer pulses and activated at less depolarized values (*b*).

is clear from the plots that this current deactivated quickly on repolarization and did not affect the measurement of $I_{ADP}$.

### $I_{ADP}$ is a chloride current

The chloride dependence of $I_{ADP}$ was investigated by measuring the reversal potential for the current and by studying the effects of changing the extracellular chloride concentration. The reversal potential for $I_{ADP}$ was measured in twenty-five cells impaled with 3 M KCl-filled electrodes using a two-pulse protocol (Fig. 4*A*) as previously described (Sánchez-Vives & Gallego, 1994). The extrapolated reversal potentials varied between −44 and 2 mV, with a mean of $-24 \pm 3{\cdot}5$ mV, which is similar to the value found with chloride-filled microelectrodes in axotomized rat sympathetic neurones (Sánchez-Vives & Gallego, 1994) and in parasympathetic ganglion cells of the rabbit (Akasu *et al.* 1990).

When some of the NaCl of the extracellular solution was replaced by sodium isethionate ($n = 4$) or sucrose ($n = 7$) the amplitude of the current increased (Fig. 4*B*, inset) and the reversal potential shifted to more positive values in accordance with the Nernst equation for chloride changes (Fig. 4*B*). These results indicate that $I_{ADP}$ is carried mostly by chloride ions, without a significant contribution from sodium ions since the replacement of NaCl by sucrose should have shifted the reversal potential in the opposite direction.

Further evidence for the chloride dependence of $I_{ADP}$ was obtained using the chloride channel blocker 9AC (Baron, Pacaud, Loirand, Mironneau & Mironneau, 1991). As shown in Fig. 4*Ca*, 2 mM 9AC produced a 75% decrease in $I_{ADP}$ (control, $-1{\cdot}1 \pm 0{\cdot}3$ nA; 9AC, $-0{\cdot}3 \pm 0{\cdot}1$ nA; $n = 4$; $P < 0{\cdot}05$, paired $t$ test) without significantly affecting $I_{peak}$. When recording in current clamp, 2 mM 9AC decreased the amplitude of the ADP produced by a train of action potentials (Fig. 4*Cb*) from a control value of $11 \pm 4$ mV to $-6 \pm 4$ mV ($n = 10$; $P < 0{\cdot}001$, paired $t$ test), without significantly affecting the resting membrane potential (control, $-52 \pm 1{\cdot}7$ mV; 9AC, $-55 \pm 1{\cdot}5$ mV). Niflumic acid at a concentration of 75 μM (White & Aylwin, 1990) also decreased $I_{ADP}$ (67% reduction; $n = 4$), but was accompanied by a significant inhibition of $I_{peak}$ (not shown).

In the rat, a calcium-dependent potassium current (Belluzzi & Sacchi, 1990; Sacchi *et al.* 1995), which is relatively resistant to TEA and blocked by apamin (Kawai & Watanabe, 1986), is responsible for the AHP observed after action potential firing. Most mouse ganglion cells showed a long AHP after the spike, suggesting that this current was also present. In accordance with this, 0·1 μM apamin enhanced the amplitude of $I_{ADP}$ (Fig. 5*A*) to $-1{\cdot}2 \pm 0{\cdot}3$ nA from a control value of $-0{\cdot}9 \pm 0{\cdot}3$ nA ($n = 5$; $P < 0{\cdot}05$,

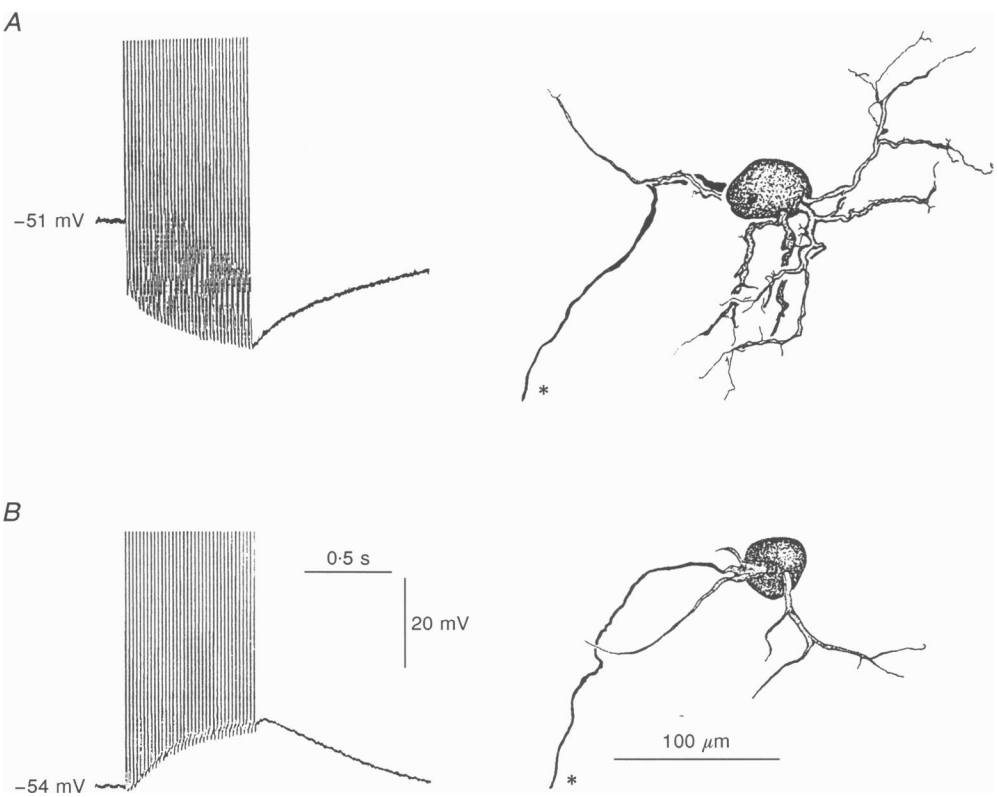


**Figure 7. After-potentials and dendritic geometry in normal sympathetic ganglion cells**

*A*, AHP recorded after a train of 35 spikes in the cell with multiple long dendrites shown on the right. $V_m$, −51 mV. *B*, ADP generated by the same stimulus in the cell with only two main dendrites shown on the right. $V_m$, −54 mV. Calibration bars apply to both panels. Asterisks indicate the axons.

paired $t$ test) and increased the ADP evoked in current clamp by a train of spikes (Fig. 5*B*) to 6 ± 5 mV from a control of −7 ± 5 mV ($n = 6$; $P < 0{\cdot}005$, paired $t$ test; $V_m$ in control solution, −56 ± 3·9 mV; $V_m$ in apamin, −55 ± 3·7 mV). Thus, calcium entry produced by spike firing or by depolarizing voltage jumps activates not only $I_{ADP}$ but also a small potassium current.

### Dendritic location of $I_{ADP}$

As stated in the Introduction, the channels responsible for $I_{ADP}$ could be located in the dendrites. In agreement with this interpretation we found a shift in the $I$–$V$ relationship for $I_{ADP}$ with depolarizing pulses of increasing duration (Fig. 6). With longer pulses $I_{ADP}$ increased in amplitude and duration (Fig. 6*A*; see also Sánchez-Vives & Gallego, 1994) and activated at more negative values, whereas $I_{peak}$ had similar amplitudes and activated at the same voltage level (Fig. 6*B*). With 25 ms pulses $I_{ADP}$ could be detected at −15 mV, whereas it was clearly present at −20 mV with 50 ms pulses and activated at around −30 mV with 200 ms pulses. One interpretation of these results is that the channels responsible for calcium entry are closer to the cell body, where the electrode is probably located, than those channels producing the $I_{ADP}$. Thus, larger depolarizations would be needed to reach a given calcium concentration in distal regions with short pulses than with long pulses.

If this view is correct, one should expect a correlation between the presence and magnitude of the ADP in a given neurone and the complexity of its dendritic tree. Therefore, in forty-nine neurones we measured the membrane potential after a train of thirty-five spikes and then stained the cells with neurobiotin. In general, neurones with a few short dendrites showed more depolarized potentials after the train. Figure 7 shows two examples, one of a cell with a marked AHP and several long dendrites (Fig. 7*A*) and the other of a neurone showing an ADP and a small dendritic tree (Fig. 7*B*). For the forty-nine cells, we found statistically significant negative correlations between the after-potential amplitude, plotted in absolute values to compensate for resting membrane potential variation, and three measures of dendritic complexity (Fig. 8): total dendritic length (Pearson correlation coefficient ($r$) = −0·343; $P = 0{\cdot}016$), number of dendritic branches 75 μm away from the cell body ($r = -0{\cdot}406$; $P = 0{\cdot}004$) and number of terminal dendrites ($r = -0{\cdot}464$; $P = 0{\cdot}001$). None of these parameters showed a significant correlation with the resting membrane potential, as shown in Fig. 8 for the number of terminal dendrites ($r = 0{\cdot}196$; $P = 0{\cdot}177$). These findings indicate that normal cells with more marked ADPs have simpler dendritic trees.

Axotomy of sympathetic neurones produces a striking dendritic retraction (Yawo, 1987) and, in the rat, the

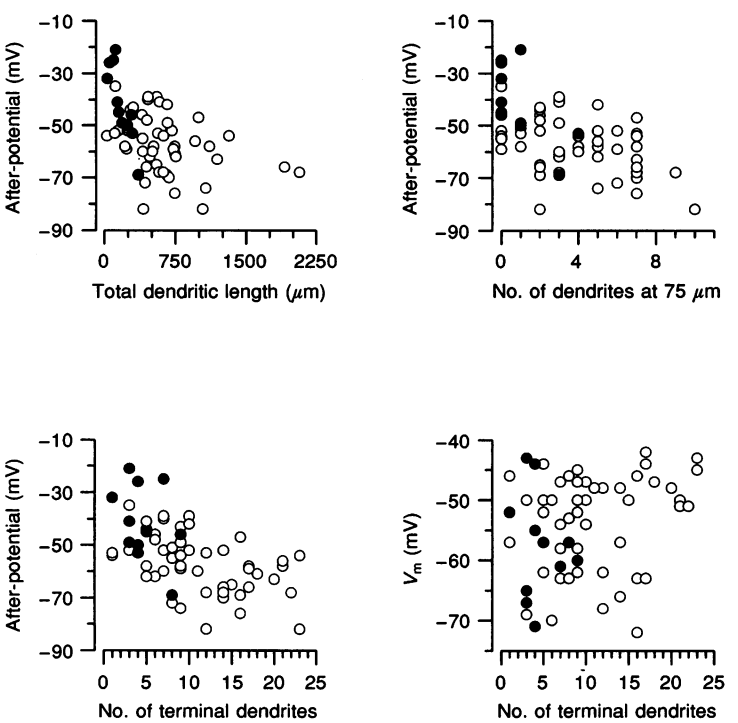


**Figure 8. Relationship between after-potential voltage and dendritic geometry**

The absolute values of the membrane potential recorded after a train of 35 spikes are plotted against three dendritic parameters measured from neurobiotin-filled cells (see Results for details). In the lower right panel resting membrane potential ($V_m$) is plotted against number of terminal dendritic segments. ○, 49 neurones from control ganglia. ●, 11 neurones from axotomized ganglia.

**Table 1. Measurements of after-potentials and dendritic parameters among sympathetic neurones**

| | Resting membrane potential (mV) | After-potential (mV) | Total dendritic length ($\mu$m) | No. of dendrites at 75 $\mu$m | No. of terminal dendrites |
|---|---|---|---|---|---|
| Control ($n = 49$) | $-53 \pm 1$ | $-57 \pm 2$ | $628 \pm 58$ | $3{\cdot}9 \pm 0{\cdot}4$ | $11{\cdot}2 \pm 0{\cdot}8$ |
| Axotomized ($n = 11$) | $-57 \pm 3$ | $-42 \pm 4$* | $177 \pm 32$* | $0{\cdot}9 \pm 0{\cdot}4$* | $4{\cdot}6 \pm 0{\cdot}7$* |

After-potentials were measured as absolute voltage values at the end of a train of 35 spikes at 50 Hz. Values are given as means $\pm$ S.E.M. * $P < 0{\cdot}001$, different from control ($t$ test).

appearance of ADPs (Sánchez-Vives & Gallego, 1993). Therefore, we investigated whether sectioning the postganglionic branches 8 days before the experiment resulted in more marked ADPs in mouse ganglion cells. Neurones were more difficult to impale and hold in operated ganglia (see also Sánchez-Vives & Gallego, 1993) but, when good recordings were obtained, ADPs were present in practically every cell and had larger amplitudes and durations than those seen in control neurones (Fig. 9, compare with Figs 1, 3, 5 and 7). Of forty-three neurones recorded with KCl-filled electrodes in operated ganglia ($V_m = -56 \pm 1{\cdot}4$ mV), 39 (91%) showed an ADP after a single spike (Fig. 9*A*), in contrast with only 3% for control ganglia. Furthermore, in all but two of thirty-four neurones tested, spike trains elicited large ADPs ($20 \pm 2$ mV; $P < 0{\cdot}001$ when compared with control cells) that lasted several seconds in many cases (Fig. 9*B*).

In eleven other cells from operated ganglia we measured the membrane potential after a train of spikes and then injected the cells with neurobiotin. The values for these cells are plotted as filled circles in Fig. 8, where it can be seen that most of them are positioned near the upper left corner of the distributions. Therefore, axotomized neurones showed large ADPs and small dendritic trees. The mean values for all the parameters presented in Fig. 8 were significantly different in cells from operated ganglia when compared with control cells (Table 1), except for the resting membrane potential. These results agree with the hypothesis that the dendritic retraction produced by axotomy brings the channels responsible for $I_{ADP}$ electrically closer to the recording electrode.

## DISCUSSION

Calcium-activated chloride currents were first observed in experiments on rod photoreceptors (Bader, Bertrand & Schwartz, 1982) and *Xenopus* oocytes (Miledi, 1982). Since then they have been identified in several neurone types (for reviews see Mayer, Owen & Barker, 1990; Scott, Sutton, Griffin, Stapleton & Currie, 1995), including spinal neurones (Owen *et al.* 1984; Hussy, 1992), primary sensory neurones (Mayer, 1985), parasympathetic neurones (Bader, Bertrand & Schlichter, 1987; Akasu *et al.* 1990) and olfactory neurones (Kleene & Gesteland, 1991). Our results show that a calcium-activated chloride current is also present in normal sympathetic ganglion cells from the mouse, where it generates an ADP after repetitive spike firing. In contrast, this current is only detected after axotomy of sympathetic ganglion cells in the rat (Sánchez-Vives & Gallego, 1994).

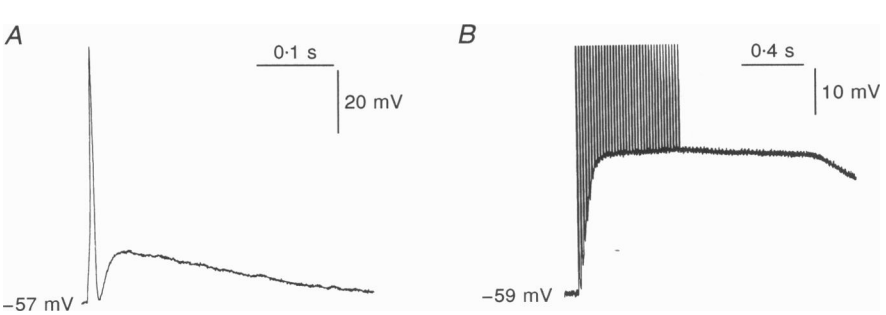


**Figure 9. ADP in axotomized neurones**

*A*, a single action potential was followed by an ADP in a neurone recorded 8 days after sectioning the postganglionic branches. $V_m$, −57 mV. *B*, in another cell from an operated ganglion a train of 35 spikes evoked a very large ADP that lasted several seconds (spikes are truncated). $V_m$, −59 mV.

Recently, a chloride current, regulated synergistically by calcium and muscarinic receptor activation, has been described in rat sympathetic ganglion cells (Marsh, Trouslard, Leaney & Brown, 1995), but as these authors point out, it is unlikely that this new current is responsible for the ADP because its activation is delayed several seconds after the rise in intracellular calcium.

The $I_{ADP}$ recorded in mouse sympathetic neurones had similar characteristics to the calcium-activated chloride current observed in axotomized superior cervical ganglion cells from the rat (Sánchez-Vives & Gallego, 1994) and in other neurones (Mayer *et al.* 1990; Scott *et al.* 1995): slow and sustained activation with depolarization, dependence on calcium and slow turn-off on repolarization. It is probable that the activation of the current directly reflects the rise in intracellular calcium concentration near the chloride channels, which only close when resting calcium levels are restored (Currie, Wooton & Scott, 1995). This is indicated by the long-lasting tail currents and ADPs, especially after axotomy (Fig. 9) when the recovery of resting calcium levels after activity is slowed down (Sánchez-Vives, Valdeolmillos & Gallego, 1993). The −24 mV reversal potential for the $I_{ADP}$ measured with KCl-filled microelectrodes was probably displaced positively by chloride leak into the cell. However, of the forty-two cells impaled with acetate-filled electrodes, twenty showed ADPs that ranged from 2 to 24 mV, with a mean of 9 mV. Therefore, the potential generated by $I_{ADP}$ is probably depolarizing under normal conditions. Furthermore, if the chloride channels are located in the dendrites, the depolarization reached there should be larger than that recorded in the soma. In this regard, the equilibrium potential calculated on the basis of intracellular chloride concentration measurements in rat sympathetic ganglion cells is around −30 mV (Ballanyi, Grafe, Reddy & ten Bruggencate, 1984; Galvan, Dörge, Beck & Rick, 1984).

The effect of apamin on the $I_{ADP}$ indicates that a residual potassium current is activated simultaneously with $I_{ADP}$, even in the presence of 25 mM TEA. This current is probably $I_{AHP}$, a calcium-dependent potassium current responsible for the slow AHP of rat sympathetic ganglion cells (Kawai & Watanabe, 1986; Sacchi *et al.* 1995). In the absence of potassium channel blockers, calcium entry during action potential firing activates both a potassium and a chloride current; the resultant potential change would therefore depend on the relative magnitude of both currents. Thus, probably all mouse ganglion cells, even those not showing ADPs, possess $I_{ADP}$ that would make the after-potential recorded in the soma more or less depolarized depending on its amplitude.

We have previously suggested that the channels responsible for the ADP are located in the distal dendrites and that the effect of their activation on the membrane potential recorded in the cell body would be inversely related to the length of the dendrites (Sánchez-Vives & Gallego, 1993, 1994). This would explain the absence of ADPs in normal ganglion cells from the rat and guinea-pig, which have long dendrites, and their presence in cells from the mouse, which have significantly shorter dendrites (Purves & Lichtman, 1985). After the marked dendritic retraction produced by axotomy (Fig. 8 and Table 1; see also Yawo, 1987), the activation of $I_{ADP}$ could be detected not only in mouse sympathetic neurones, where practically all axotomized cells exhibit ADPs, but also in rat ganglion cells. However, the longer dendrites of guinea-pig ganglion cells would still impede the detection of $I_{ADP}$ from the cell body after axotomy (Sánchez-Vives & Gallego, 1993). Of course it is possible that other processes occur after axotomy that could explain the effect on the ADP, such as expression or redistribution of ion channels, changes in intracellular calcium levels, or changes in channel dynamics.

However, there are two more facts that favour a dendritic location for $I_{ADP}$. One is the shift in the $I$–$V$ relationship for the activation of $I_{ADP}$ with pulses of increasing duration (Fig. 6). Although there are other explanations, e.g. a larger calcium entry making the currents visible at less depolarized voltage levels, this shift would be expected if chloride channels are localized away from those that allow calcium entry. If this was the case, short pulses should be of large amplitude to produce calcium levels high enough to activate the chloride channels. This does not imply that the chloride channels must be located in the dendrites, but it is certainly compatible with this idea. One should expect that, in axotomized neurones, which have shorter dendrites, the shift in voltage level for the activation of $I_{ADP}$ would disappear, or at least decrease. We tried to test this point but axotomized cells deteriorated quickly under the voltage-clamp conditions needed to run the protocol. One fact favouring a separate location for calcium and chloride channels is that, in cultured dorsal root ganglion cells without processes, the calcium-dependent chloride current reaches maximum amplitude with 100 ms pulses (Currie & Scott, 1992), whereas in our experiments pulses of more than 200 ms had to be applied to maximally activate $I_{ADP}$.

Another factor in support of a dendritic location for $I_{ADP}$ is the negative correlation between the amplitude of the after-potential and three measures of dendritic tree complexity (Fig. 8). The correlation coefficients are statistically significant at the 1% level for the number of terminal dendrites and of dendrites longer than 75 $\mu$m and at the 5% level for the total dendritic length, although the degree of correlation is low. Even without the two extreme points at the right in the upper graphs of Fig. 8, these correlations are still significant at the 5% level. Furthermore, if the data from axotomized and control neurones are pooled, the correlations become stronger: $r = -0{\cdot}474$, $P = 0{\cdot}0002$ (total dendritic length); $r = -0{\cdot}534$, $P = 0{\cdot}00001$ (number of dendrites 75 $\mu$m away from the cell body); $r = -0{\cdot}538$, $P = 0{\cdot}00001$ (number of terminal dendritic segments). Therefore our data indicate that in mouse sympathetic

neurones the presence of ADPs is associated with few short dendrites, which agrees with the idea that normal ganglion cells from the rat and guinea-pig do not show ADPs because of their long dendrites. Of course correlation does not imply causation, but until the difficulties in obtaining recordings directly from the dendrites are overcome, the hypothesis of a dendritic location for the chloride channels responsible for $I_{ADP}$ is compatible with the available data.

The function of the calcium-activated chloride current in neurones is not known (Scott *et al.* 1995). Because its activation produces a depolarization in several neurone types, it is possible that this current increases membrane excitability after action potential firing. However, the simultaneous activation of $I_{AHP}$ and $I_{ADP}$ in sympathetic ganglion cells probably increases the membrane conductance so much that excitability is decreased. This agrees with the phasic firing of most rat superior cervical ganglion cells when depolarized with intracellular currents (for a review, see Adams & Harper, 1995) and with the fact that the cells in our experiments did not fire spontaneously during the ADPs (see also Sánchez-Vives & Gallego, 1994). If the channels responsible for the ADP are indeed located in the dendrites, their activation could have important consequences for synaptic transmission since most synaptic contacts are made there (Forehand, 1985).


Adams, D. J. & Harper, A. A. (1995). Electrophysiological properties of autonomic ganglion neurons. In *Autonomic Ganglia*, ed. McLachlan, E. M., pp. 153–212. Harwood Academic Publishers, Luxembourg.

Akasu, T., Nishimura, T. & Tokimasa, T. (1990). Calcium-dependent chloride current in neurones of the rabbit pelvic parasympathetic ganglia. *Journal of Physiology* **422**, 303–320.

Bader, C. R., Bertrand, D. & Schlichter, R. (1987). Calcium-activated chloride current in cultured sensory and parasympathetic quail neurones. *Journal of Physiology* **394**, 125–148.

Bader, C. R., Bertrand, D. & Schwartz, E. A. (1982). Voltage-activated and calcium-activated currents studied in solitary rod inner segments from the salamander retina. *Journal of Physiology* **331**, 253–284.

Ballanyi, K., Grafe, P., Reddy, M. M. & ten Bruggencate, G. (1984). Different types of potassium transport linked to carbachol and $\gamma$-aminobutyric acid actions in rat sympathetic neurons. *Neuroscience* **12**, 917–927.

Baron, A., Pacaud, P., Loirand, G., Mironneau, C. & Mironneau, J. (1991). Pharmacological block of $Ca^{2+}$-activated $Cl^-$ current in rat vascular smooth muscle cells in short-term primary culture. *Pflügers Archiv* **419**, 553–558.

Belluzzi, O. & Sacchi, O. (1986). A quantitative description of the sodium current in the rat sympathetic neurone. *Journal of Physiology* **380**, 275–291.

Belluzzi, O. & Sacchi, O. (1989). Calcium currents in the normal adult rat sympathetic neurone. *Journal of Physiology* **412**, 493–512.

Belluzzi, O. & Sacchi, O. (1990). The calcium-dependent potassium conductance in rat sympathetic neurones. *Journal of Physiology* **422**, 561–583.

Currie, K. P. M. & Scott, R. H. (1992). Calcium-activated currents in cultured neurones from rat dorsal root ganglia. *British Journal of Pharmacology* **106**, 593–602.

Currie, K. P. M., Wooton, J. F. & Scott, R. H. (1995). Activation of $Ca^{2+}$-dependent $Cl^-$ currents in cultured rat sensory neurones by flash photolysis of DM-nitrophen. *Journal of Physiology* **482**, 291–307.

De Castro, F., Geijo-Barrientos, E. & Gallego, R. (1995*a*). A calcium-dependent chloride current in mouse sympathetic neurons. *Society for Neuroscience Abstracts* **21**, 2032.

De Castro, F., Sánchez-Vives, M. V., Muñoz-Martinez, E. J. & Gallego, R. (1995*b*). Effects of postganglionic nerve section on synaptic transmission in the superior cervical ganglion of the guinea-pig. *Neuroscience* **67**, 689–695.

Forehand, C. J. (1985). Density of somatic innervation on mammalian autonomic ganglion cell is inversely related to dendritic complexity and preganglionic convergence. *Journal of Neuroscience* **5**, 3403–3408.

Galvan, M., Dörge, A., Beck, F. & Rick, R. (1984). Intracellular electrolyte concentrations in rat sympathetic neurones measured with an electron microprobe. *Pflügers Archiv* **400**, 274–279.

Hussy, N. (1992). Calcium-activated chloride channels in cultured embryonic *Xenopus* spinal neurons. *Journal of Neurophysiology* **68**, 2042–2050.

Kawai, T. & Watanabe, M. (1986). Blockade of Ca-activated K conductance by apamin in rat sympathetic neurones. *British Journal of Pharmacology* **87**, 225–232.

Kleene, S. J. & Gesteland, R. C. (1991). Calcium-activated chloride conductance in frog olfactory cilia. *Journal of Neuroscience* **11**, 3624–3629.

McAfee, D. A. & Yarowsky, P. J. (1979). Calcium-dependent potentials in the mammalian sympathetic neurone. *Journal of Physiology* **290**, 507–523.

Marsh, S. J., Trouslard, J., Leaney, J. L. & Brown, D. A. (1995). Synergistic regulation of a neuronal chloride current by intracellular calcium and muscarinic receptor activation: a role for protein kinase C. *Neuron* **15**, 729–737.

Mayer, M. L. (1985). A calcium-activated chloride current generates the after-depolarization of rat sensory neurones in culture. *Journal of Physiology* **364**, 217–239.

Mayer, M. L., Owen, D. G. & Barker, J. L. (1990). Calcium-dependent chloride currents in vertebrate central neurons. In *Chloride Channels and Carriers in Nerve, Muscle and Glial Cells*, ed. Alvarez-Leefmans, F. J. & Russell, J. M., pp. 355–364. Plenum Press, New York and London.

Miledi, R. (1982). A calcium-dependent transient outward current in *Xenopus* oocytes. *Proceedings of the Royal Society* B **315**, 491–497.

Morgan, C. W., de Groat, W. C., Felkins, L. A. & Zhang, S. J. (1991). Axon collaterals indicate broad intraspinal role for sacral preganglionic neurons. *Proceedings of the National Academy of Sciences of the USA* **88**, 6888–6892.

Owen, D. G., Segal, M. & Barker, J. L. (1984). A Ca-dependent $Cl^-$ conductance in cultured mouse spinal neurones. *Nature* **311**, 567–570.

Purves, D. (1975). Functional and structural changes in mammalian sympathetic neurones following interruption of their axons. *Journal of Physiology* **252**, 429–463.

PURVES, D. & LICHTMAN, J. W. (1985). Geometric differences among homologous neurons in mammals. *Science* **228**, 298–302.

SACCHI, O., ROSSI, M. L. & CANELLA, R. (1995). The slow $Ca^{2+}$-activated $K^+$ current, $I_{AHP}$, in the rat sympathetic neurone. *Journal of Physiology* **483**, 15–27.

SÁNCHEZ-VIVES, M. V. & GALLEGO, R. (1993). Effects of axotomy or target atrophy on membrane properties of rat sympathetic ganglion cells. *Journal of Physiology* **471**, 801–815.

SÁNCHEZ-VIVES, M. V. & GALLEGO, R. (1994). Calcium-dependent chloride current induced by axotomy in rat sympathetic neurons. *Journal of Physiology* **475**, 391–400.

SÁNCHEZ-VIVES, M. V., VALDEOLMILLOS, M. & GALLEGO, R. (1993). Changes in intracellular calcium control induced by axotomy in sympathetic neurones. *Pflügers Archiv* **424**, R63.

SCHOFIELD, G. G. & IKEDA, S. R. (1989). Sodium and calcium currents of acutely isolated adult rat superior cervical ganglion neurons. *Pflügers Archiv* **411**, 481–490.

SCOTT, R. H., SUTTON, K. G., GRIFFIN, A., STAPLETON, S. R. & CURRIE, K. P. M. (1995). Aspects of calcium-activated chloride currents: a neuronal perspective. *Pharmacology and Therapeutics* **66**, 535–565.

WHITE, M. M. & AYLWIN, M. (1990). Niflumic and flufenamic acids are potent reversible blockers of $Ca^{2+}$-activated $Cl^-$ channels in *Xenopus* oocytes. *Molecular Pharmacology* **37**, 720–724.

YAWO, H. (1987). Changes in dendritic geometry of mouse superior cervical ganglion cells following postganglionic axotomy. *Journal of Neuroscience* **7**, 3703–3711.

**Acknowledgements**

We are indebted to Drs J. V. Sánchez Andrés and M. Valdeolmillos for their comments on the manuscript and to Messrs S. Moya and A. Pérez-Vegara for expert technical assistance. This work was supported by grants PB92-0347 and PM95-0107 from the Dirección General de Investigación Científica y Técnica (Spain).

**Author's email address**

R. Gallego: gallegor@ua.es

*Received 20 August 1996; accepted 17 October 1996.*